



Electrical, structural, and electrochemical studies on novel nanocomposite polymer electrolyte $\text{PEO}_{30}\text{NaC}_{12}\text{H}_{25}\text{SO}_4-x \text{ wt.}\% \text{Fe}_2\text{O}_3$

D. Joice Sheeba¹ · Josephine Sangeetha Gerald¹ · K. Venkatesh¹

Received: 30 May 2024 / Revised: 29 July 2024 / Accepted: 11 August 2024
© The Author(s), under exclusive licence to Springer-Verlag GmbH Germany, part of Springer Nature 2024

Abstract

Ion-conducting thin nanocomposite polymer electrolyte films were prepared by solution casting technique using poly (ethylene oxide) (PEO) and sodium lauryl sulfate ($\text{NaC}_{12}\text{H}_{25}\text{SO}_4$) salt complexation in the ratio 30:1. Fine nanoparticles of iron(III) oxide (Fe_2O_3) were incorporated into the polymer matrix at various weight percentages. The XRD pattern exhibited the amorphous nature of the novel nanocomposite polymer electrolyte thin films, and FTIR studies showed the complexation and the incorporation of the nanoparticles in the polymer matrix. The maximum ionic conductivity of $3.76 \times 10^{-6} \text{ Scm}^{-1}$ was obtained for the sample with 5 wt.% of Fe_2O_3 . Thermal and morphological studies showed a reduction in the degree of crystallinity of the polymer material. The electrochemical cell was fabricated at room temperature (304 K) using the chosen best conducting thin nanocomposite polymer film with an open circuit voltage (OCV) of 1.255 V and a short circuit current (SCC) of 648 μA .

Keywords Poly (ethylene oxide) · Sodium-ion conduction · Nanocomposite polymer electrolyte · Cell parameters

Introduction

In the era of scientific advancements, there is always room for more and more improvements in the currently available resources that make our lives much simpler and easier. Ion-conducting thin film batteries find their way into mini portable electronic devices such as supercapacitors, smart cards, and cellular telephones [1, 6]. Their applications may be further extended in the fabrication of high-energy batteries, fuel cells, photochemical cells, electrochemical display devices, and chemical sensors [2, 3]. Polymer electrolyte films have promising applications in the above-discussed fields, due to their relative ease in fabrication, high ionic conductivity, and almost zero electronic conductivity accompanied with high energy density [4, 5]. Polymeric electrolytes form compact and flexible solid-state structures devoid of leaks and come with different geometries to meet the desired requirements [1]. PEO has been a major subject of interest in polymer electrolytic applications, where the transient cross-links

between the cations and ether oxygen of PEO play a significant role in facilitating ion dissociation. A good electrolyte is characterized by effective electrode–electrolyte contacts, wide electrochemical stability, and electrochemical compatibility with electrode material [2].

For an appreciable conductivity of the polymer electrolyte, it is necessary to increase the volume fraction of the polymer's amorphous phase. This may be obtained by the incorporation of plasticizers, ceramic fillers like SiO_2 , ZnO , etc., and the addition of salts in order to reduce the crystalline nature of the polymer electrolyte, facilitating an improved conductivity [5].

PEO is chosen as the polymer host due to its high dielectric constant, solvating ability, compatibility with electrodes, ease of processing, and relatively cost-effective. It has excellent thermal and mechanical stability and a high electrochemical window. However, the high crystallinity of PEO at room temperature can restrict chain mobility and limit ionic conductivity, which is addressed by adding salts, nanofillers, or modifying its structure to increase the amorphous nature [6]. Sodium lauryl sulfate is chosen as a salt dopant for the fabrication of sodium-ion batteries. When compared to other sodium salts, Sodium lauryl sulfate provides a favorable combination of the large sulfate anion and small sodium cation, which creates an ionic environment

✉ D. Joice Sheeba
joicesheeba@mcc.edu.in

¹ Department of Physics, Madras Christian College affiliated to University of Madras, East Tambaram, Chennai 600 059, India

that enhances the mobility and transport of charge carriers in the solid polymer electrolyte system. Fe_2O_3 is chosen as a nanofiller. Incorporating Fe_2O_3 nanoparticles can reduce the level of crystallinity in the polymer, hence impacting the glass transition temperature (T_g) and improving the ionic mobility and overall conductivity of the polymer electrolyte system [7].

In the present investigation, ion-conducting nanocomposite polymer electrolyte films were obtained by the incorporation of sodium lauryl sulfate salt into PEO along with different weight percentages of nanoparticles of iron(III) oxide. Various characterization techniques such as X-ray diffraction (XRD), Fourier transform infrared spectroscopy (FTIR), complex impedance spectroscopy, temperature study, differential scanning calorimetry (DSC), and scanning electron microscopy (SEM) were carried out to support the discussion. Furthermore, the dielectric properties of the best-conducting nanocomposite polymer electrolyte were determined.

Materials and methods

Stand-alone nanocomposite polymer electrolyte thin films were prepared by the solution casting technique. Commercially available salt of sodium lauryl sulfate $\text{NaC}_{12}\text{H}_{25}\text{SO}_4$ ($M_w = 288.38$ g/mol) was added to poly (ethylene oxide) of molecular weight ($M_w = 5 \times 10^6$ kg mol⁻¹, Aldrich). Fe_2O_3 nanoparticles (NP size < 50 nm, $M_w = 159.69$ g/mol, Aldrich) were dispersed into the polymer matrix without any further chemical treatments. Using a magnetic stirrer, a stoichiometric amount of PEO was made to dissolve in the solvent of acetonitrile until it formed a uniform homogenous medium. The calculated amount of sodium lauryl sulfate was then added to the homogenous PEO solution and stirred well at the room temperature of ~ 303 K to form a salt complexation. Once the homogeneity was achieved, iron(III) oxide nanoparticles (Fe_2O_3) at different weight percentages were dispersed into the matrix and stirred uniformly until it became homogenous. The homogenous mixture was then transferred onto vacuum-treated borosilicate glass Petri dishes which were dried at 328 K.

Characterization techniques

The thin films were analyzed to determine the ionic conductivity using a Hioki IM 3536 LCR meter. The impedance was measured over frequencies ranging between 100 Hz and 4 MHz by applying the magnitude of 0.5 V. The electrical conductivity values were obtained using the following formula:

$$\sigma = t/R_b A (\text{S cm}^{-1}) \quad (1)$$

where “ t ” is the thickness of the sample, R_b is the bulk resistance of the material that is determined from the intercept formed at the real axis of the impedance plot, and “ A ” is the surface area of the sample that makes contact with the sample holder.

Temperature studies using the same setup were carried out to study the variation in the conductivity from room temperature (~ 304 K) up to 328 K for every 5 K rise in temperature. The nanocomposite polymer electrolyte thin films were studied using X-ray diffraction spectroscopy (XRD) (Rich Seifert, GE XRD 3000TT, operating at a voltage of 40 kV and a current of 30 mA in the range between 10 and 90° with a step size of 0.1°) to obtain the peaks of PEO in order to confirm its presence and to explain the reduction in the intensity of the peak due to the increased amorphous nature of the polymer electrolyte. FTIR measurements on a SHIMADZU IRAffinity-1 spectrometer in the range 400–4000 cm⁻¹ with a spectral resolution of 2 cm⁻¹ were done to study the interaction between the polymer–salt–nanoparticles and to provide information on cation–oxygen interactions in a wide range of PEO-metal salt systems. Differential scanning calorimetry (DSC) thermogram was recorded using NETZSCH DSC 214 at a heating rate of 5 °C/min in the temperature range from 20 to 90 °C under nitrogen atmosphere instrument was done in order to determine the phase transition and the decrease in the degree of crystallinity which plays a major role in the enhancement of ionic conductivity. The structural morphology of the best conducting polymer-based thin film was obtained using the FEI-Quanta FEG 200F scanning electron microscopy (SEM) with × 10 k magnification at 30 kV electron beam.

The best conducting nanocomposite polymer electrolyte was employed in the making of miniature sodium-ion batteries. The battery was fabricated using the sodium metal made in the form of a small pellet of thickness ~ 1 mm as the anode and a mixture of iodine (I_2) + carbon (C) + the obtained electrolyte taken in the ratio 3:3:1 made into a pellet of thickness ~ 2 mm as the cathode.

X-ray diffraction analysis

Qualitative identification of the complexation of sodium lauryl sulfate salt in pure PEO matrix was determined using the X-ray diffraction studies, along with various magnitudes of dispersion of Fe_2O_3 nanoparticles at room temperature.

X-ray diffraction pattern of pure PEO and nanocomposite polymer electrolyte, $\text{PEO}_{30}\text{NaC}_{12}\text{H}_{25}\text{SO}_{4-x}$ wt.% Fe_2O_3 are shown in Fig. 1. From the XRD pattern, it can be inferred

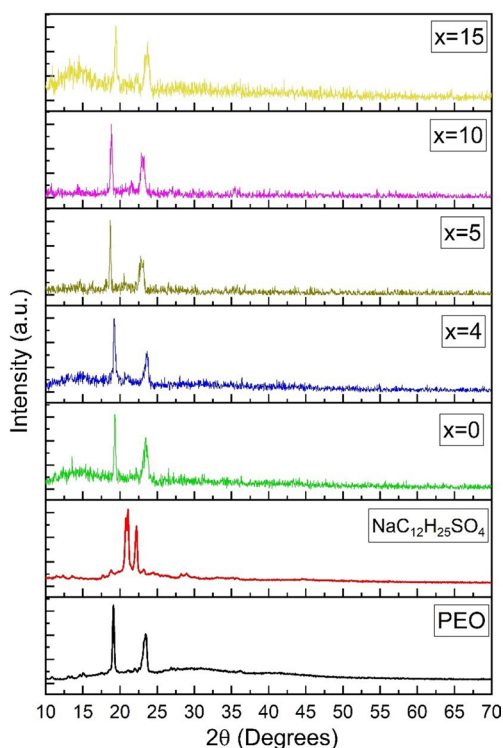


Fig. 1 X-ray diffraction pattern of pure PEO, $\text{NaC}_{12}\text{H}_{25}\text{SO}_4$ salt, and $\text{PEO}_{30}\text{NaC}_{12}\text{H}_{25}\text{SO}_4-x$ wt.% Fe_2O_3 nanocomposite electrolyte films

that peaks occurring between $2\theta = 18^\circ$ and 25° refers to the characteristic peaks of the host polymer PEO [5, 8].

A slight shift in the characteristic peaks of PEO was observed in the addition of sodium lauryl sulfate salt. Furthermore, no new significant peaks were observed on the incorporation of sodium lauryl sulfate salt (which has two major peaks at $2\theta = 21^\circ$ and 22° and a minor peak at $2\theta = 28^\circ$) to the PEO host. This reveals that a good complexation was achieved between PEO and the sodium lauryl sulfate salt [9]. From Fig. 1, it is evident that salt complexed polymer electrolyte exhibits a decrease in the peak intensity, indicating a decrease in the crystalline nature of pure PEO. The intensity was further abridged by the incorporation of Fe_2O_3 nanoparticles, thereby increasing its amorphous nature.

Gradual change in the characteristic peaks may be observed for higher weight percentages (10 wt.%, 15 wt.%) of Fe_2O_3 nanoparticles. This implies that the degree of crystallinity increased due to the aggregation of nanoparticles, thereby decreasing its amorphous nature. This may create a major hindrance to the mobility of Na^+ ions, narrowing down its electrical conductivity [5, 10]. The crystallite size (L) of the PEO samples was calculated using the Debye–Scherrer equation [11]

$$L = \frac{0.94\lambda}{\beta \cos\theta} \quad (2)$$

where λ is the wavelength of the X-ray (1.540 \AA), β is the full-width half minimum of the peak, and θ is the Bragg diffraction angle. The calculated values are listed in Table 1.

Fourier-transform infrared spectroscopic analysis

High spectral resolution data over a wide range of spectra offered by FTIR spectroscopy is used to study the interactivity between the polymer, salt, and nanoparticles. A comparison graph showing the FTIR results of $(\text{PEO}_{30}\text{NaC}_{12}\text{H}_{25}\text{SO}_4-x \text{ wt.\% Fe}_2\text{O}_3)$ is shown in Fig. 2.

The strong absorption band occurring between 2962 and 2800 cm^{-1} characterizes the strong asymmetric C–H

Table 1 The value of Bragg's angle, full-width half maxima, and crystalline size for pure PEO and $\text{PEO}_{30}\text{NaC}_{12}\text{H}_{25}\text{SO}_4-x$ wt.% Fe_2O_3 electrolytes

x wt.% Fe_2O_3	$\theta(^{\circ})$	$\beta(^{\circ})$	L (nm)
PEO	19.11	0.250	33.6
	23.36	0.53	15.9
0	19.28	0.26	32.3
	23.44	0.54	15.5
4	19.2	0.28	29.2
	23.68	0.58	14.5
5	18.67	0.29	28.3
	22.87	0.61	13.7
10	18.85	0.26	31.3
	23.05	0.568	14.8
15	19.44	0.25	33.1
	23.72	0.565	14.9

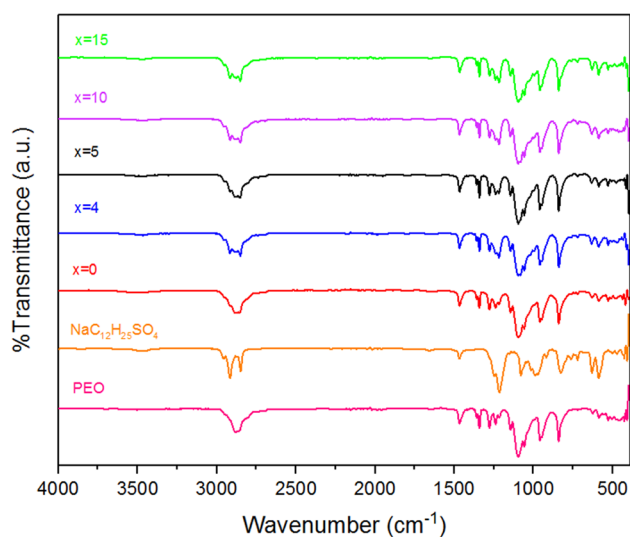


Fig. 2 FTIR spectrum corresponding to pure PEO, salt, and $\text{PEO}_{30}\text{NaC}_{12}\text{H}_{25}\text{SO}_4-x$ wt.% Fe_2O_3 nanocomposite electrolyte films

stretching vibrations of the CH₂ group of PEO [5, 12]. The peaks occurring between 1520 and 1400 cm⁻¹ correspond to the CH₂ scissoring mode. The peak appearing at 1342 cm⁻¹ corresponds to the CH₂ bending. The characteristic peak of CH₂ symmetric twisting occurs at approximately 1238 cm⁻¹. The peak at 1100 cm⁻¹ of pure PEO corresponds to the C–O–C stretching mode [5, 13]. Such well-resolved bands of ether oxygen groups (C–O–C) in the chemical structure of the polymer chain indicate that PEO is compatible or soluble with other materials [13]. The peak at 1146 cm⁻¹ corresponds to the C–C stretching. The peak at 840 cm⁻¹ corresponds to the C–O stretching in PEO. The peaks occurring between 800 and 1000 cm⁻¹ correspond to the rocking modes of CH₂. The spectral lines occurring between 960 and 840 cm⁻¹ for all nanocomposite polymer electrolytes including pure PEO correspond to the symmetrical and asymmetrical rocking mode of CH₂, which is unaltered by complexation with salt as well as the dispersion of Fe₂O₃ nanoparticles [13]. This indicates the gauche confirmation of O–[(CH₂)₂]–O [5, 13].

For further analysis, a detailed FTIR study was done on sodium lauryl sulfate salt. The FTIR spectrum of sodium lauryl sulfate shows two prominent peaks at 1220 cm⁻¹ and 1108 cm⁻¹, which corresponds to the asymmetric and symmetric stretching of the S=O, respectively [5, 14]. The peaks corresponding to the Fe–O stretching occur between 627 and 476 cm⁻¹ [15, 16]. The addition of various weight percentages of Fe₂O₃ nanoparticles characterizes the decrease in the intensity of the spectral lines and the slight broadening of the bands were observed. Such observation suggests that the competition between Fe₂O₃ and oxygen atoms with respect to Na⁺ ions makes oxygen atoms act with H atoms, which relatively decreases the CH₂ and C–O–C absorptions. A slight shift in the prominent peaks confirms the interaction between PEO and NaC₁₂H₂₅SO₄ and Fe₂O₃.

Differential scanning calorimetry analysis

DSC studies were carried out in order to acquire the thermal properties of PEO, PEO₃₀NaC₁₂H₂₅SO₄–*x* wt.% Fe₂O₃ (*x*=0, 5) polymer electrolytes. The degree of crystallinity may be calculated using the melting enthalpy (ΔH_m) of the polymer electrolyte and the melting enthalpy (ΔH_m^ϕ) of the 100% pure crystalline material PEO from the following formula:

$$X_c = (\Delta H_m / \Delta H_{m^\phi}) \times 100\% \quad (3)$$

Table 2 gives the melting enthalpy ΔH_m and the degree of crystallinity X_c of the polymer electrolytes [17]. The melting peak (T_m) of the pure PEO occurs at 65.2 °C which is in good agreement with the standard reported value [17–19]. The exothermic peak of salt complexed PEO electrolyte PEO₃₀NaC₁₂H₂₅SO₄ occurs at 65.9 °C. Subsequently, the

Table 2 Melting enthalpy ΔH_m and the degree of crystallinity X_c of the polymer electrolytes

Polymer electrolyte	ΔH_m (J/g)	X_c (%)	T_m (°C)
PEO	203.265	98.7	65.2
PEO ₃₀ NaC ₁₂ H ₂₅ SO ₄	118.808	58.4	65.9
PEO ₃₀ NaC ₁₂ H ₂₅ SO ₄ –5 wt.% Fe ₂ O ₃	31.5777	15.53	64.9

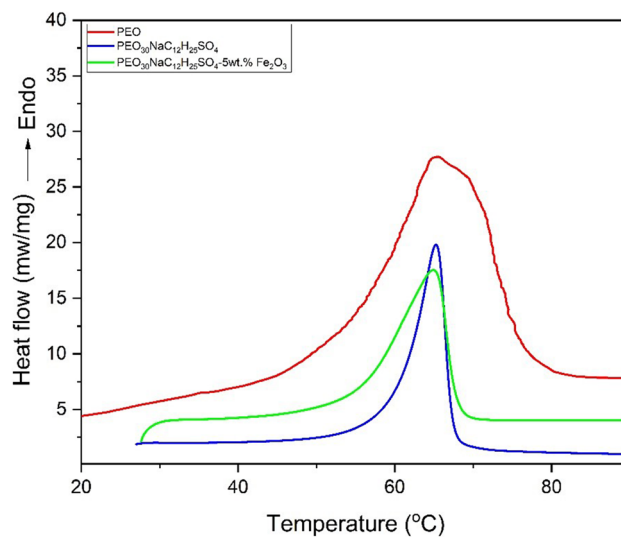


Fig. 3 DSC plot for PEO, PEO₃₀NaC₁₂H₂₅SO₄, and PEO₃₀NaC₁₂H₂₅SO₄–5 wt.% Fe₂O₃ polymer electrolytes

degree of crystallinity is seen to decrease with the addition of sodium lauryl sulfate salt, from 98.2 to 58.4% [5].

The degree of crystallinity further drops to 15.53% with the addition of 5 wt.% of Fe₂O₃ nanoparticles with a slight shift in the exothermic peak from 65.9 to 64.9 °C. Figure 3 shows a considerable reduction in the intensity of the melting peaks of the polymer electrolytes. This may be attributed to the increase in the amorphous nature, which contributes to the enhancement in the ionic conductivity due to the increased flexibility of the polymer chains [5].

Electrical conductivity analysis

Figure 4 shows the AC electrical conductivity of the nanocomposite polymer electrolyte at room temperature (304 K), evaluated from the complex impedance spectrum. The semi-circular regions at high frequencies provide information such as the bulk resistance (R_b) and bulk capacitance (C_b) of the nanocomposite polymer electrolyte. The vertical spike at lower frequencies may be due to dielectric relaxation and ion trapping in the complex network contributing to additional resistance and capacitance [5, 8].

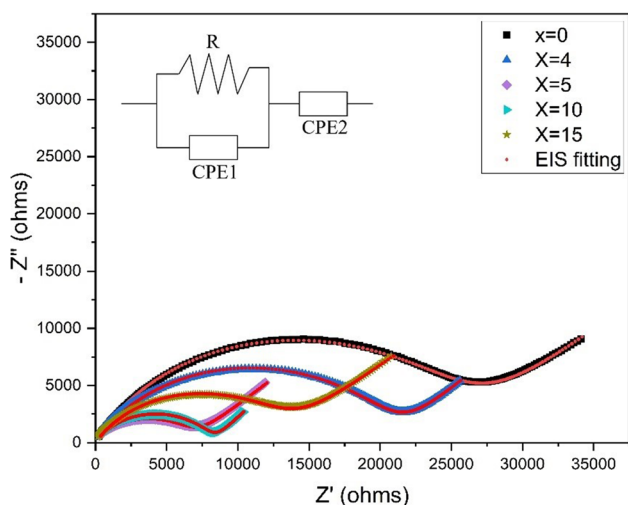


Fig. 4 Nyquist plot of various weight percentages $\text{PEO}_{30}\text{NaC}_{12}\text{H}_{25}\text{SO}_4-x$ wt.% Fe_2O_3 at room temperature (304 K)

The EIS spectrum analyzer software has been used to estimate the bulk resistance (R_b) and other fitting parameters of the polymer electrolytes. The values of conductivity and fitted parameters for various weight percentages of Fe_2O_3 nanoparticles in the salt-complexed PEO matrix ($\text{PEO}_{30}\text{NaC}_{12}\text{H}_{25}\text{SO}_4-x$ wt.% Fe_2O_3) at room temperature are given in Table 3.

The electrical conductivity of pure PEO at observed room temperature is found to be $\sigma_{(304\text{ K})} = 7.255 \times 10^{-9} \text{ Scm}^{-1}$. A considerable increase in the electrical conductivity by two orders is observed on the incorporation of salt to the host PEO matrix $\sigma_{(304\text{ K})} = 9.02 \times 10^{-7} \text{ Scm}^{-1}$. Further enhancement in the order of electrical conductivity is observed after the uniform dispersion of Fe_2O_3 nanoparticles in the salt complexed polymer matrix $\sigma_{(304\text{ K})} = 3.76 \times 10^{-6} \text{ Scm}^{-1}$. A reduction in the conductivity is observed when the concentration of Fe_2O_3 nanoparticles is increased above the optimum level (i.e., 5 wt.% Fe_2O_3).

This may be ascribed to excessive nanoparticle concentration in the solid polymer electrolyte, leading to ion pairs and ion aggregation, inhibiting ionic conduction and slowing

down its mobility [20, 21]. Figure 5 shows the variation in ionic conductivity as a function of various wt.% of Fe_2O_3 of solid polymer electrolyte.

Temperature studies and activation energy measurements

Impedance measurements of ($\text{PEO}_{30}\text{NaC}_{12}\text{H}_{25}\text{SO}_4-x$ wt.% Fe_2O_3) at various temperatures (304–328 K) were studied. Table 4 gives the values of conductivity for various weight percentages of Fe_2O_3 nanoparticles in the salt complexed PEO matrix ($\text{PEO}_{30}\text{NaC}_{12}\text{H}_{25}\text{SO}_4-x$ wt.% Fe_2O_3) at temperatures 308 to 328 K.

The dependence of ionic conductivity of the nanocomposite polymer electrolyte at various weight percentages of Fe_2O_3 nanoparticles reveals that the ionic conductivity is thermally activated with an increase in temperature. Thereby, the conductivity of the nanocomposite polymer electrolyte tends to increase with the increase in temperature

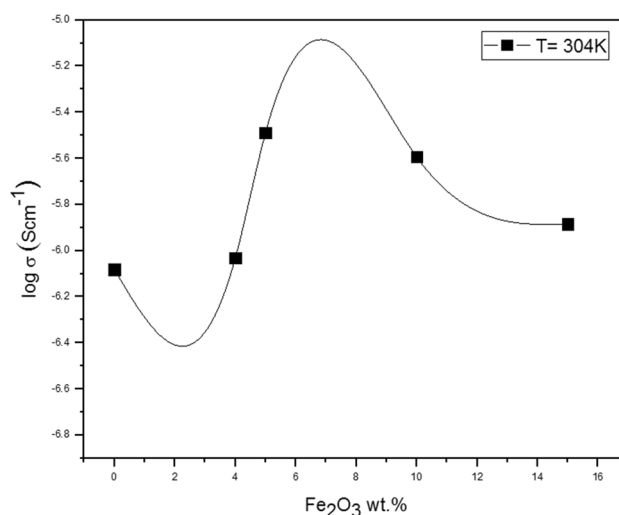


Fig. 5 Variation in ionic conductivity as a function of nanoparticle weight percentage

Table 3 The electrical conductivity values and fitting parameters for various weight percentages of Fe_2O_3 nanoparticles in the salt-complexed PEO matrix ($\text{PEO}_{30}\text{NaC}_{12}\text{H}_{25}\text{SO}_4-x$ wt.% Fe_2O_3) at room temperature

x wt.%	Thickness (cm)	R_b (K Ω)	Electrical conductivity σ (Scm^{-1}) at 304 K	CPE1 (F)	CPE2 (F)	n1 (no unit)	n2 (no unit)
0	0.015	25.1	9.02×10^{-7}	6.85×10^{-9}	3.46×10^{-6}	0.70	0.48
4	0.013	20.9	9.77×10^{-7}	7.08×10^{-9}	4.86×10^{-6}	0.69	0.52
5	0.016	6.68	3.76×10^{-6}	1.68×10^{-8}	5.80×10^{-6}	0.66	0.48
10	0.015	8.26	2.86×10^{-6}	1.11×10^{-8}	7.77×10^{-6}	0.68	0.56
15	0.012	12.83	1.47×10^{-6}	1.36×10^{-8}	4.41×10^{-6}	0.69	0.46

Table 4 Conductivity for various weight percentages of Fe₂O₃ nanoparticles in (PEO₃₀NaC₁₂H₂₅SO₄-x wt.% Fe₂O₃) at temperatures at 308 to 328 K

x wt.%	308 K		313 K		318 K		323 K		328 K	
	R _b (KΩ)	Electrical conductivity σ (Scm ⁻¹)	R _b (KΩ)	Electrical conductivity σ (Scm ⁻¹)	R _b (KΩ)	Electrical conductivity σ (Scm ⁻¹)	R _b (KΩ)	Electrical conductivity σ (Scm ⁻¹)	R _b (KΩ)	Electrical conductivity σ (Scm ⁻¹)
0	26.3	8.965 × 10 ⁻⁷	22	1.072 × 10 ⁻⁶	19.5	1.209 × 10 ⁻⁶	16.5	1.429 × 10 ⁻⁶	13	1.814 × 10 ⁻⁶
4	21	9.730 × 10 ⁻⁷	17.6	1.161 × 10 ⁻⁶	14.8	1.380 × 10 ⁻⁶	12	1.703 × 10 ⁻⁶	8.9	2.296 × 10 ⁻⁶
5	7.5	3.353 × 10 ⁻⁶	6.8	3.698 × 10 ⁻⁶	5.3	4.745 × 10 ⁻⁶	4.35	5.781 × 10 ⁻⁶	3.5	7.186 × 10 ⁻⁶
10	9	2.619 × 10 ⁻⁶	7.5	3.144 × 10 ⁻⁶	6.45	3.656 × 10 ⁻⁶	5	4.716 × 10 ⁻⁶	4	5.895 × 10 ⁻⁶
15	14.25	1.324 × 10 ⁻⁶	12	1.572 × 10 ⁻⁶	9.5	1.965 × 10 ⁻⁶	8	2.358 × 10 ⁻⁶	6	3.144 × 10 ⁻⁶

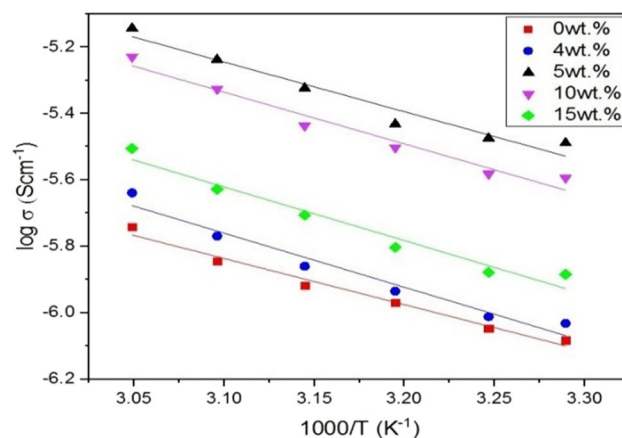


Fig. 6 Arrhenius plot of the nanocomposite polymer electrolyte thin film (PEO₃₀NaC₁₂H₂₅SO₄-x wt.% Fe₂O₃) at various temperatures

Table 5 Values of activation energy (E_a) for (PEO₃₀NaC₁₂H₂₅SO₄-x wt.% Fe₂O₃)

x wt.% Fe ₂ O ₃	Activation energy E _a (eV)
0	0.1453
4	0.1400
5	0.1288
10	0.1342
15	0.1389

following the Arrhenius-type thermally activated process [21].

Figure 6 shows the Arrhenius plot of the nanocomposite polymer electrolyte thin film (PEO₃₀NaC₁₂H₂₅SO₄-x wt.% Fe₂O₃) at various temperatures. Activation energy is the combination of defect formation energy and migration energy which is calculated from the slope of the conductivity against a 1000/T plot [22]. The values of the activation energy for (PEO₃₀NaC₁₂H₂₅SO₄-x wt.% Fe₂O₃) are listed in Table 5.

The activation energy at various weight percentages of Fe₂O₃ nanoparticles were listed in Table 5, that the lowest value of activation energy (0.1288 eV) is obtained for 5 wt.% of Fe₂O₃ which is the best-conducting nanocomposite polymer electrolyte exhibiting high ionic conductivity [23, 24]. The activation energy tends to increase with the increase in the concentration of Fe₂O₃ nanoparticles above the optimum concentration, indicating the aggregation of ions.

Scanning electron microscopy analysis

SEM micrograph showing the structural morphology of pure PEO is shown in Fig. 7.

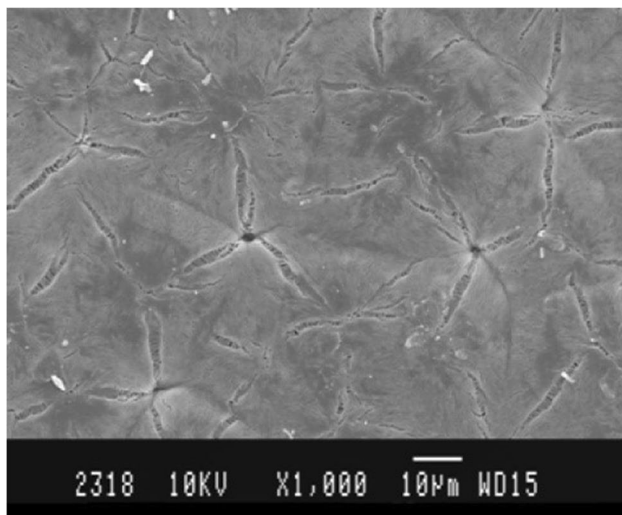


Fig. 7 SEM micrograph of pure PEO thin film

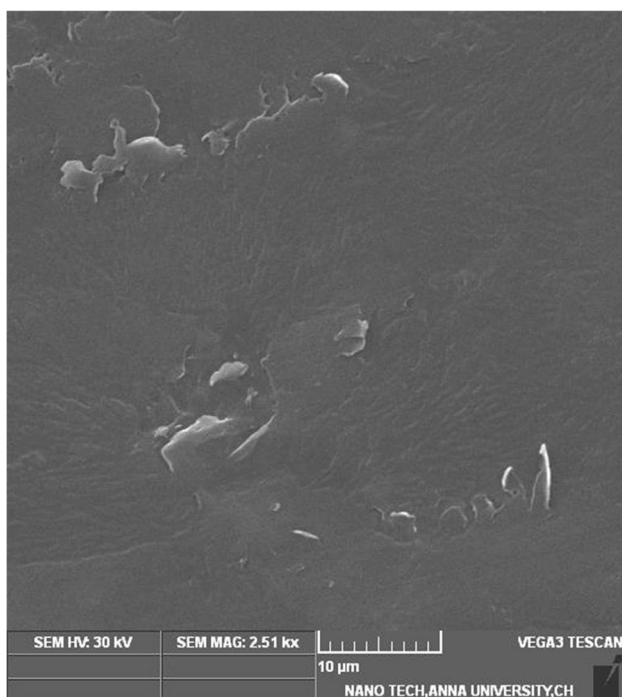


Fig. 8 SEM micrograph of $\text{PEO}_{30}\text{NaC}_{12}\text{H}_{25}\text{SO}_4$

It is observed from the figure that orderly arranged prominent spherulites of similar size are recorded in the SEM micrograph of pure PEO. This depicts the crystalline nature of the pure PEO thin film [25]. Figure 8 (magnification of $\times 10$ k), shows a considerable improvement from the crystalline to amorphous nature as an outcome of the addition of sodium lauryl sulfate salt into the PEO membrane. The absence of crystalline spherulites in the salt-complexed polymer electrolyte film $\text{PEO}_{30}\text{NaC}_{12}\text{H}_{25}\text{SO}_4$ shows

that the presence of salt inhibits the crystalline nature of PEO [5]. An enhancement in the structural morphology is observed with the addition of Fe_2O_3 nanoparticles to the salt-complexed PEO electrolyte thin film. The intricately arranged spherulites, no longer appear in the micrograph of $\text{PEO}_{30}\text{NaC}_{12}\text{H}_{25}\text{SO}_4$ -5 wt.% Fe_2O_3 film.

Figure 9a (magnification of $\times 10$ k) SEM micrograph also shows that Fe_2O_3 nanoparticles are randomly distributed within the salt-complexed polymer matrix, having no surface contact between them but with good interfacial bonding.

Figure 9b (magnification of $\times 8$ k) shows the boundary separation of larger regions and the pores. This unique pattern is attributed to the amorphous nature of the nano-composite polymer electrolyte thin film, which facilitates enhanced ionic conductivity.

Dielectric constant and dielectric loss analysis

In a given volume of the polymer electrolyte, the amount of dipole alignment can be calculated using the dielectric constant (ϵ').

$$\epsilon' = C_p t / \epsilon_0 A \quad (4)$$

where C_p is the parallel capacitance, t is the thickness of the sample, ϵ_0 is the permittivity of the free space and A is the area of the sample under study. The value of ϵ' is higher at low frequency in comparison to the high-frequency region. This may be attributed to the space charge buildup near the electrode–electrolyte interface, which hinders the mobility of the charges. The value of ϵ' is seen to decrease with increasing frequencies before reaching a constant value. This can be due to the inability of the dipoles in the macromolecules to orient themselves in the direction of the applied electric field [21, 26].

The dielectric loss (ϵ'') is the loss of energy during the ion motion and dipole alignment when there is a rapid reversal in the polarity of the electric field. It is determined using the following formula:

$$\epsilon'' = \sigma / \omega \epsilon_0 \quad (5)$$

where σ is the ionic conductivity, and ω is the angular frequency.

The higher and lower values of ϵ'' at lower and higher frequencies depend upon the availability of time for the charges to build up at the interface. At lower frequencies, the charges are sufficiently built up at the interface before the polarity reversal. However, at higher frequencies, the buildup of charges occurs only at the boundaries of the conducting species and at the ends of the conducting path [21].

The increase in the temperature facilitates the dissociation of ion pairs which causes an increase in the

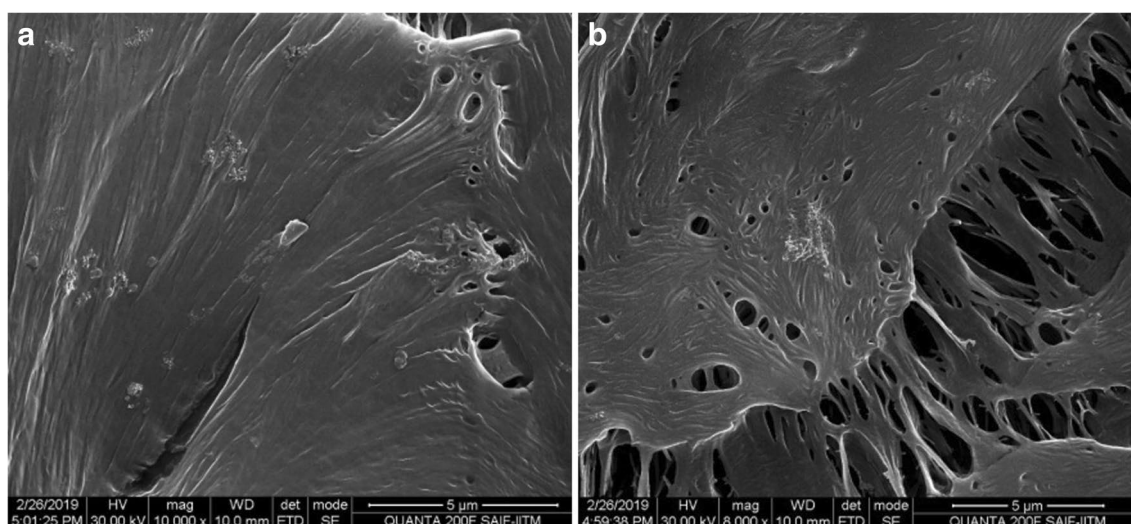


Fig. 9 a and b SEM micrographs of (PEO₃₀NaC₁₂H₂₅SO₄-5 wt.% Fe₂O₃)

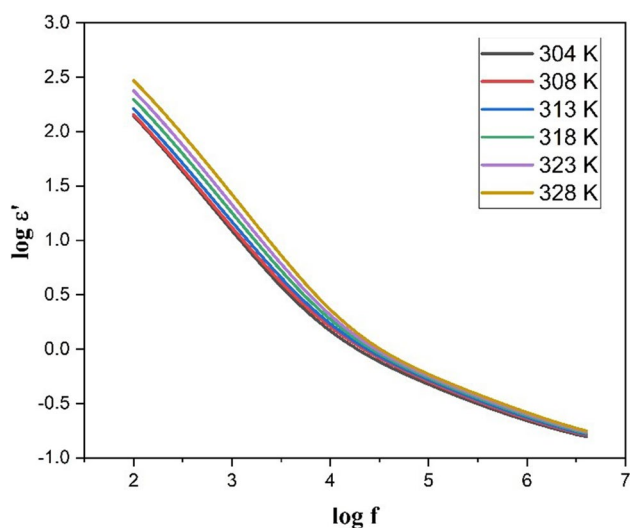


Fig. 10 Variation of the dielectric constant (ϵ') for PEO₃₀NaC₁₂H₂₅SO₄-5 wt.% Fe₂O₃

concentration of free charge carriers at the interface. High temperature also prevents ion aggregation and formation of ion clusters in the nanocomposite polymer electrolyte thus allowing it to retain its amorphous nature. It also increases the parallel capacitance by forming a space charge region, which exhibits a high dielectric constant [21]. It is evident from Figs. 10 and 11 that both ϵ' and ϵ'' show similar behaviors with frequency at various temperatures. The absence of relaxation peaks indicates that the increase in conductivity was predominantly due to the increase in the number of mobile ions in PEO₃₀NaC₁₂H₂₅SO₄-5 wt.% Fe₂O₃.

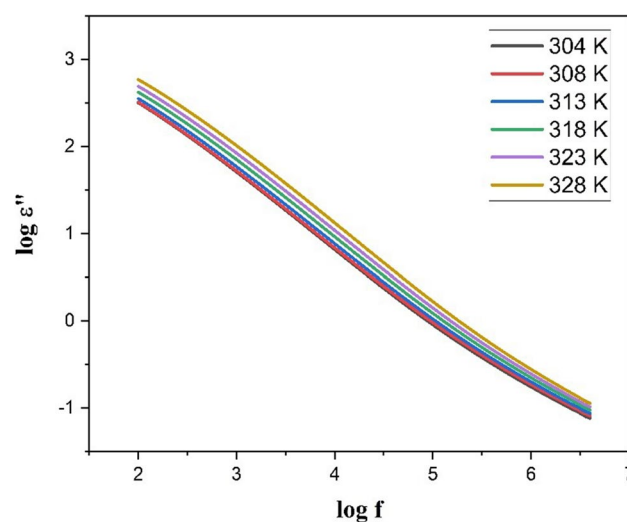


Fig. 11 Variation in the dielectric loss (ϵ'') for PEO₃₀NaC₁₂H₂₅SO₄-5 wt.% Fe₂O₃

Loss tangent analysis

The loss tangent analysis (δ) as a function of frequency is used to determine the dielectric relaxation parameter of the nanocomposite polymer electrolyte. It is the ratio of the dielectric loss (ϵ'') of the material to its dielectric constant (ϵ').

$$\tan \delta = \sigma / \omega \epsilon_0 \quad (6)$$

It measures the ratio of the electric energy lost to the energy stored in an applied electric field. Figure 12 shows that δ increases for a particular range of frequencies before reaching the maximum after which it is seen to decrease

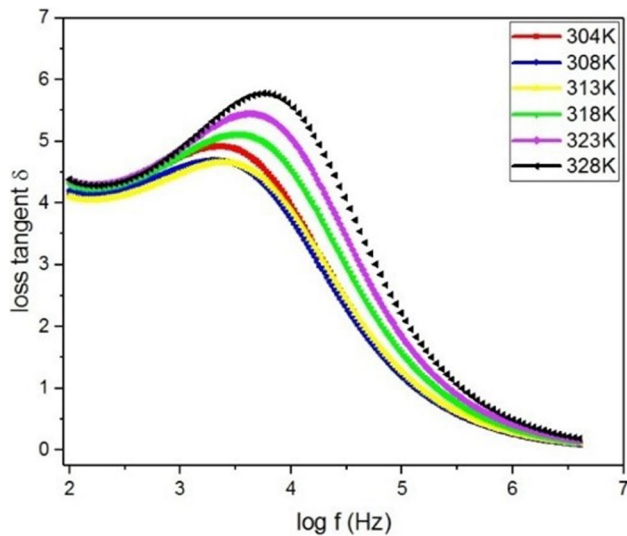


Fig. 12 Variation of the loss tangent (δ) as a function of frequency, for the best conducting nanocomposite polymer electrolyte from room temperature (304 K) to 328 K

rapidly. The peaks acquired at various temperatures correspond to the electrode polarization frequency. The peak frequency is inversely proportional to the relaxation time of the ions. The peak position is seen to shift toward the higher frequency as the temperature increases. This leads to an increased ionic conductivity due to the decrease in the relaxation time [21].

Electric modulus analysis

The dielectric behavior of the best-conducting nanocomposite polymer electrolyte was further studied with the help of electric modulus analysis. The conductivity relaxation process and the ion hopping mechanism may be determined from the electric modulus analysis spectra.

The real part of the electric modulus (M') is determined from the formula [21].

$$M' = \epsilon' / (\epsilon'^2 + \epsilon''^2) \tag{7}$$

where ϵ' is the dielectric constant, and ϵ'' is the dielectric loss.

From Fig. 13, it is quite evident that M' approaches zero at lower frequencies indicating that there is a negligible contribution of the electrode polarization. M' is found to increase gradually at higher frequencies and the dispersion observed in that region may be due to the spreading of the conductivity relaxation over the range of frequencies [26]. It is also evident that the modulus spectra overlap at various temperatures which indicates that the distribution of the relaxation times is independent of temperatures. This also

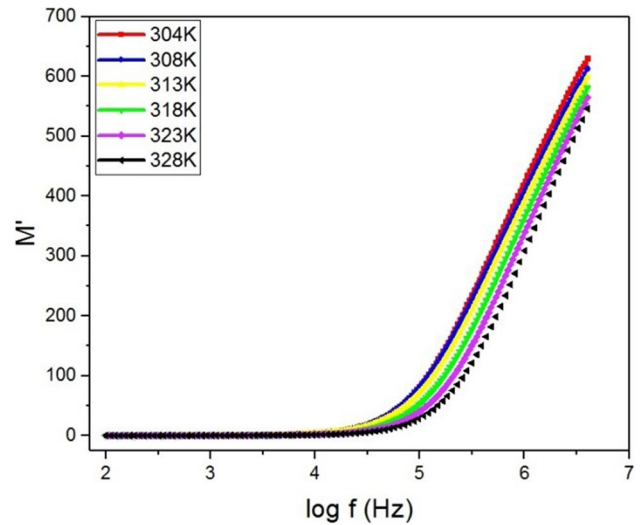


Fig. 13 Variation of the real modulus (M') as a function of frequency, for the best conducting nanocomposite polymer electrolyte from room temperature (304 K) to 328 K

shows the brilliant electrochemical stability of the nanocomposite polymer electrolyte [21].

The imaginary part of the electric modulus (M'') is determined using the formula [21].

$$M'' = \epsilon'' / (\epsilon'^2 + \epsilon''^2) \tag{8}$$

The values of M'' as seen in Fig. 14 seem to decrease as the frequency decreases, indicating the negligible contribution of the electrode polarization to the electric modulus [26].

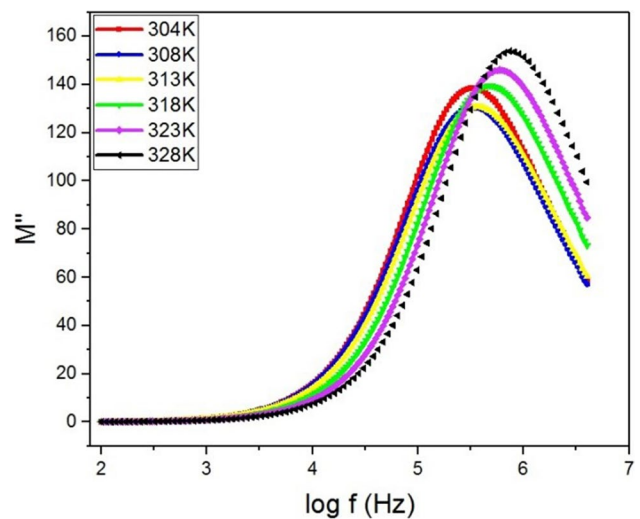


Fig. 14 Variation of the imaginary modulus (M'') as a function of frequency, for the best conducting nanocomposite polymer electrolyte from room temperature (304 K) to 328 K

The increase in the values of M'' at higher frequencies corresponds to the long-range random hopping of the ions in the nanocomposite polymer electrolyte, which reaches a maximum at a particular frequency. The peaks so observed may be attributed to the ionic conductivity relaxation process in the nanocomposite polymer electrolyte thin film, where the long-range motion is limited down to confined motion. The peaks also confirm that the nanocomposite polymer electrolyte is an ionic conductor [22]. The asymmetry and the broadening of the peak may be attributed to the non-Debye behavior [21, 26]. Further decrease in M'' at much higher frequencies may indicate that the charge carriers are mobile over only short distances [21].

The peak positions appear to be shifted toward the higher frequency side as the temperature is increased. This elucidates the mobility of the charge carriers becoming rapid due to the increased flexibility of the nanocomposite polymer electrolyte at elevated temperatures.

Battery studies

The obtained nanocomposite polymer electrolyte possessed the maximum ionic conductivity and good thermal stability. These characteristics offer a promising candidate for replacing lithium-ion batteries with sodium-ion batteries in portable electronic devices [27].

In order to evaluate the electrochemical performance of $\text{PEO}_{30}\text{NaC}_{12}\text{H}_{25}\text{SO}_4-5 \text{ wt.}\% \text{Fe}_2\text{O}_3$, a prototype battery was fabricated with the configuration of $\text{Na} | \text{PEO}$ electrolyte $| \text{C} + \text{I}_2 + \text{polymer electrolyte}$ as cathode and sodium metal as anode, as depicted by Fig. 15. Figure 16 shows the OCV and discharge through $1 \text{ M}\Omega$ of the electrochemical cell fabricated with the same configuration. It is evident from the figure that a discharge plateau is observed for 33 h. The cell parameters including the open circuit voltage (OCV) short

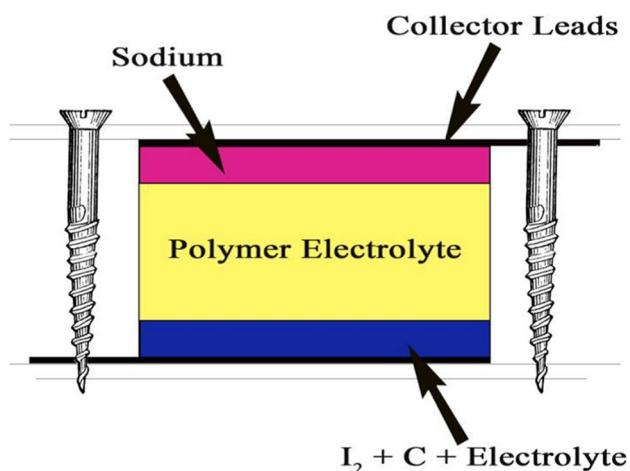


Fig. 15 Schematic diagram of an electrochemical cell

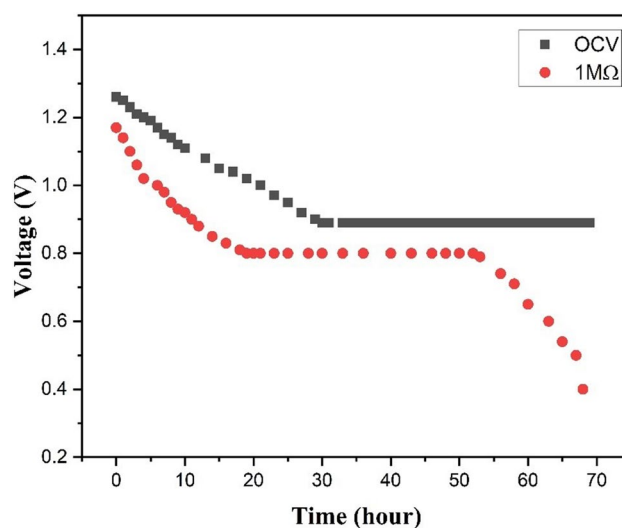


Fig. 16 OCV and discharge plot of the fabricated battery

circuit current (SCC), and other evaluated cell parameters recorded at room temperature (304 K) are tabulated and presented in Table 6.

Conclusion

The interactions between Fe_2O_3 nanoparticles, the polymer chains, and the ions produced as the result of the dissociation of salt were confirmed by several characterizations. Good complexation of sodium lauryl sulfate ($\text{NaC}_{12}\text{H}_{25}\text{SO}_4$) with the ether oxygen of PEO has been confirmed through FTIR studies. The reduced area of melting enthalpy in the DSC studies, in addition to Fe_2O_3 nanoparticles, indicated the reduction in the crystalline nature of the nanocomposite polymer electrolyte. SEM analysis showed the absence of periodic spherulite structure in the nanocomposite polymer electrolyte which were quite prominently seen in the crystalline domains of pure PEO. The ionic conductivity of the

Table 6 Cell parameters of $\text{PEO}_{30}\text{NaC}_{12}\text{H}_{25}\text{SO}_4-5 \text{ wt.}\% \text{Fe}_2\text{O}_3$

Cell parameters	5 wt.% Fe_2O_3
Weight (g)	1.15
Area (cm^2)	1.13
Open circuit voltage (V)	1.255
Short circuit current (μA)	648
Current density ($\mu\text{A}/\text{cm}^2$)	573.45
Power density (W/Kg)	0.719
Time of plateau region (h)	33
Discharge capacity (mAh)	21.38
Energy density (Wh/Kg)	23.73

nanocomposite polymer electrolyte $\text{PEO}_{30}\text{NaC}_{12}\text{H}_{25}\text{SO}_4-5$ wt.% Fe_2O_3 is $3.76 \times 10^{-6} \text{ Scm}^{-1}$, which is three orders more than that of the pure polymer. Excellent dielectric properties along with other prominent characteristics make $\text{PEO}_{30}\text{NaC}_{12}\text{H}_{25}\text{SO}_4-5$ wt.% Fe_2O_3 a propitious material for the development of solid-state batteries for the application on ambient temperature devices. A miniature electrochemical cell was fabricated at room temperature (304 K) using the best-conducting polymer electrolyte which gave an open circuit voltage of 1.255 V and short circuit current of 648 μA . The present investigation has thus demonstrated the development of a new Na^+ -ion-conducting PEO-based novel nanocomposite polymer electrolytes appropriate for ambient temperature applications.

Acknowledgements University Grants Commission (F. No. 4-4/2015-16) (MRP/UGCSERO), Hyderabad and DST-FIST, UGC-CPE, Madras Christian College, Tambaram 59.

Author contribution Dr. D. Joice Sheeba—Corresponding author—Concept and Analysis. Josephine Sangeetha Gerald—Manuscript writing, tables, Figures. Both of us are involved in writing and investigating Venkatesh K—Tables, Figures.

Funding The author D. Joice Sheeba is thankful to the University Grants Commission (F. No. 4-4/2015-16) (MRP/UGCSERO), Hyderabad and DST-FIST, UGC-CPE, Madras Christian College, Tambaram for providing financial assistance.

Data availability Available on request.

Declarations

Conflict of interest The authors declare no competing interests.

References

- Ghosh A, Kofinas P (2008) PEO based block copolymer as solid state lithium battery electrolyte. *ECS Trans* 11(29):131–137. <https://doi.org/10.1149/1.2938916>
- Reddeppa N, Sharma AK, Narasimha Rao VVR (2013) Wen Chen: Preparation and characterization of pure and KBr doped polymer blend (PVC/PEO) electrolyte thin films. *Microelectron Eng* 112:57–62. <https://doi.org/10.1016/j.mee.2013.05.015>
- Chun-yue P, Qing F, Li-jun W, Qian Z, Meng C (2007) Morphology and conductivity of in-situ PEO-LiClO₄-TiO₂ composite polymer electrolyte. *J Cent South Univ Technol* 14:348. <https://doi.org/10.1007/s11771-007-0069-1>
- Lin CW, Hung CL, Venkateswarlu M, Hwang BJ (2005) Influence of TiO₂ nano-particles on the transport properties of composite polymer electrolyte for lithium-ion batteries. *J Power Sources* 146:397–401. <https://doi.org/10.1016/j.jpowsour.2005.03.028>
- JoiceSheeba D (2019) Sivasankaran BR: Characteristic studies on PEO-based thin nanocomposite polymer electrolytes. *Ionics* 25:2627. <https://doi.org/10.1007/s11581-018-2799-5>
- Feng J, Wang L, Chen Y, Wang P, Zhang H, He X (2021) PEO based polymer-ceramic hybrid solid electrolytes: a review. *Nano convergence* 8:1–12
- Do NST, Schaetzel DM, Dey B, Seabaugh AC, Fullerton-Shirey SK (2012) Influence of Fe₂O₃ nanofiller shape on the conductivity and thermal properties of solid polymer electrolytes: nanorods versus nanospheres. *J Phys Chem C* 116(40):21216–21223
- Ragavendran K, Kalyani P, Veluchamy A, Banumathi S, Thirunakaran R, Benedict TJ (2004) Characterization of plasticized PEO based solid polymer electrolyte by XRD and AC impedance methods. *Port Electrochim Acta* 22:149–159. <https://doi.org/10.4152/pea.200402149>
- Xu J, Xiong Q, Liang G, Shen X, Zou H, Xu W (2009) Ion-polymer interactions in SmCl₃(H₂O)₆ doped poly(ethylene oxide) electrolytes. *J Macromol Sci Part B* 48:856–866. <https://doi.org/10.1080/00222340902958778>
- Li Z, Su G, Wang X, Gao D (2005) Micro-porous P(VDF-HFP)-based polymer electrolyte filled with Al₂O₃ nanoparticles. *Solid State Ionics* 176:1903–1908. <https://doi.org/10.1016/j.ssi.2005.05.006>
- Mohamed F, Hameed TA, Abdelghany AM, Turky G (2021) Structure–dynamic properties relationships in poly (ethylene oxide)/silicon dioxide nanocomposites: dielectric relaxation study. *Polym Bull* 78:5205–5223
- Jinisha B, Anilkumar KM, Manoj M, Abhilash A, Pradeep VS, Jayalekshmi S (2017) Poly (ethylene oxide) (PEO)-based, sodium ion-conducting, solid polymer electrolyte films, dispersed with Al₂O₃ filler, for applications in sodium ion cells. *Ionics* 24:1675. <https://doi.org/10.1007/s11581-017-2332-2>
- Kiran Kumar K, Ravi M, Pavani Y, Bhavani S, Sharma AK, Narasimha Rao VVR (2014) Investigations on PEO/PVP/NaBr complexed polymer blend electrolytes for electrochemical cell applications. *J Membr Sci* 454:200–211. <https://doi.org/10.1016/j.memsci.2013.12.022>
- Chatterjee S, Salaün F, Campagne C (2014) The influence of 1-butanol and trisodium citrate ion on morphology and chemical properties of chitosan-based microcapsules during rigidification by alkali treatment. *Mar Drugs* 12:5801–5816. <https://doi.org/10.3390/md12125801>
- Liu J, Yang H, Xue X (2019) Preparation of different shaped $\alpha\text{-Fe}_2\text{O}_3$ nanoparticles with large particles of iron oxide red. *CrystalEngComm* 21:1097–1101. <https://doi.org/10.1039/C8CE01920G>
- Kumar S, Manikandan VS, Palai AK, Mohanty S, Nayak SK (2019) Fe₂O₃ as an efficient filler in PVDF-HFP based polymeric electrolyte for dye sensitized solar cell application. *Solid State Ionics* 332:10–15
- Anantha PS, Hariharan K (2005) Physical and ionic transport studies on poly(ethylene oxide)–NaNO₃ polymer electrolyte system. *Solid State Ionics* 176:155–162. <https://doi.org/10.1016/j.ssi.2004.07.006>
- Verma ML, Sahu HD (2015) Ionic conductivity and dielectric behavior of PEO-based silver ion conducting nanocomposite polymer electrolytes. *Ionics* 21(12):3223–3231
- Yalla MR, Jeedi VR, Devi SS, Ganta KK, Reddy SN et al (2023) Influence of silica nanoparticles on structural, electrical, and dielectric properties of PEO/PVdF/NaNO₃/EC based composite solid polymer electrolytes. *NanoWorld J* 9(S4):S562–S569
- Kumar KK, Ravi M, Pavani Y, Bhavani S, Sharma AK, Narasimha Rao VVR (2011) Investigations on the effect of complexation of NaF salt with polymer blend (PEO/PVP) electrolytes on ionic conductivity and optical energy band gaps. *Phys B Condens Matter* 406:1706–1712. <https://doi.org/10.1016/j.physb.2011.02.010>
- Verma ML, Sahu HD (2017) Study on ionic conductivity and dielectric properties of PEO-based solid nanocomposite polymer electrolytes. *Ionics* 23:2339–2350. <https://doi.org/10.1007/s11581-017-2063-4>
- Mohapatra SR, Thakur AK, Choudhary RNP (2008) Studies on PEO-based sodium ion conducting composite polymer films. *Ionics* 14:255–262. <https://doi.org/10.1007/s11581-007-0171-2>

23. Yap YL, Cheang PL, You AH, Teo LL (2015) Modelling of temperature dependence on PEO electrolyte with Al_2O_3 . *Comput Mater Sci* 106:59–63
24. Karan NK, Pradhan DK, Thomas R, Natesan B, Katiyar RS (2008) Solid polymer electrolytes based on polyethylene oxide and lithium trifluoro-methane sulfonate ($\text{PEO-LiCF}_3\text{SO}_3$): ionic conductivity and dielectric relaxation. *Solid State Ionics* 179(19–20):689–696
25. Suthanthiraraj SA, Sheeba DJ (2007) Structural investigation on PEO-based polymer electrolytes dispersed with Al_2O_3 nanoparticles. *Ionics* 13:447. <https://doi.org/10.1007/s11581-007-0131-x>
26. Bhide A, HariharanK (2007) Ionic transport studies on $(\text{PEO})_6:\text{NaPO}_3$ polymer electrolyte plasticized with PEG_{400} . *Eur Polym J* 43:4253–4270. <https://doi.org/10.1016/j.eurpolymj.2007.07.038>
27. Sreepathi Rao S, Rao KVS, Shareefuddin Md, Subba Rao UV, Chandra S (1994) Ionic conductivity and battery characteristic studies on PEO+AgNO_3 polymer electrolyte. *Solid State Ionics* 67:331–334

Publisher's Note Springer Nature remains neutral with regard to jurisdictional claims in published maps and institutional affiliations.

Springer Nature or its licensor (e.g. a society or other partner) holds exclusive rights to this article under a publishing agreement with the author(s) or other rightsholder(s); author self-archiving of the accepted manuscript version of this article is solely governed by the terms of such publishing agreement and applicable law.